ELSEVIER

Journal of Alloys and Compounds 467 (2009) 450–458

Journal of ALLOYS AND COMPOUNDS

www.elsevier.com/locate/jallcom

Effect of specimen thickness on the growth rate of chromia scales on Ni-base alloys in high- and low-pO_2 gases

J. Zurek*, G.H. Meier[1], E. Essuman, M. Hänsel, L. Singheiser, W.J. Quadakkers

Forschungszentrum Jülich, IEF-2, 52428 Jülich, Germany

Received 4 October 2007; received in revised form 4 December 2007; accepted 6 December 2007
Available online 15 December 2007

Abstract

Two types of experiments were carried out to study the oxidation behaviour of NiCr-base model alloys; thermogravimetric measurements for up to 72 h exposure at 1000 °C in synthetic air and isothermal exposures for up to 100 h at 1000 °C in laboratory air and in Ar–4%H_2–2%H_2O. It was found that there is a significant effect of specimen thickness on the oxidation rate of all studied alloys. The growth rates of the chromia scales decrease with increasing specimen thickness in both air and the Ar–H_2–H_2O mixture. Based on the present results in combination with recent literature data for ferritic steels, it is postulated that the decrease in rate is the result of compressive growth stresses in the scales which can relax by plastic deformation of the substrate for thin specimens but are maintained at significant levels for thick specimens.

Keywords: High temperature alloys; SEM; Oxidation; Diffusion; Grain boundaries

1. Introduction

Many applications of high temperature alloys, particularly weight-sensitive applications require thin specimen cross-sections. It was shown for alumina forming ferritic steels that the oxidation limited lifetime of thin components is primarily governed by the Al reservoir in the component [1,2]. If the growth and re-healing of the oxide scale leads to a decrease of the alloy Al-concentration beneath a critical level, breakaway oxidation occurs. Due to the very high oxide growth rates accompanied by this event, the time at which breakaway occurs, represents the lifetime limit of the component [3,4]. As, for a given alloy, the Al reservoir decreases with decreasing component thickness, the lifetime will decrease with decreasing component thickness.

Recently it was shown that chromia forming ferritic steels also show the effect of component thickness on the lifetime at 800 and 900 °C (Fig. 1), i.e. with decreasing sample thickness the oxidation limited lifetime of the high-Cr ferritic steels decreases due to breakaway phenomena [5–7]. This effect is caused by faster exhaustion of the chromium reservoir from the bulk alloy in the case of thinner components [5]. The observed lifetime limits in the temperature range 800–900 °C can be predicted with reasonable accuracy by a similar approach to that previously used for FeCrAl alloys, using oxide growth rate parameters, initial alloy Cr content and critical Cr content required for protective chromia scale formation.

The authors observed for the ferritic steels that the growth rate of chromia base scales increased as the specimen thickness was decreased. A possible explanation given was that the thickness dependence of the scale growth rate is affected by depletion of minor alloying elements such as Mn in the bulk alloy and/or by internal oxidation, mainly of Si and Al [5]. A further explanation was that the effect is related to relaxation of oxide growth stresses during isothermal and/or cyclic exposure [6]. The effect tends to increase with increasing temperature possibly due to the strong decrease in creep strength of the ferritic steel with increasing temperature.

The thickness dependence of the oxidation rate of the chromia forming ferritic steels was found during air exposures but not in low oxygen partial pressure gases used to simulate the anode gas in a solid oxide fuel cell [7].

In the present paper the specimen thickness dependence of the isothermal oxidation behaviour of chromia forming Ni-base

---

* Corresponding author.
E-mail address: j.zurek@fz-juelich.de (J. Zurek).

[1] University of Pittsburgh, Pittsburgh, PA, USA.

0925-8388/$ – see front matter © 2007 Elsevier B.V. All rights reserved.
doi:10.1016/j.jallcom.2007.12.015

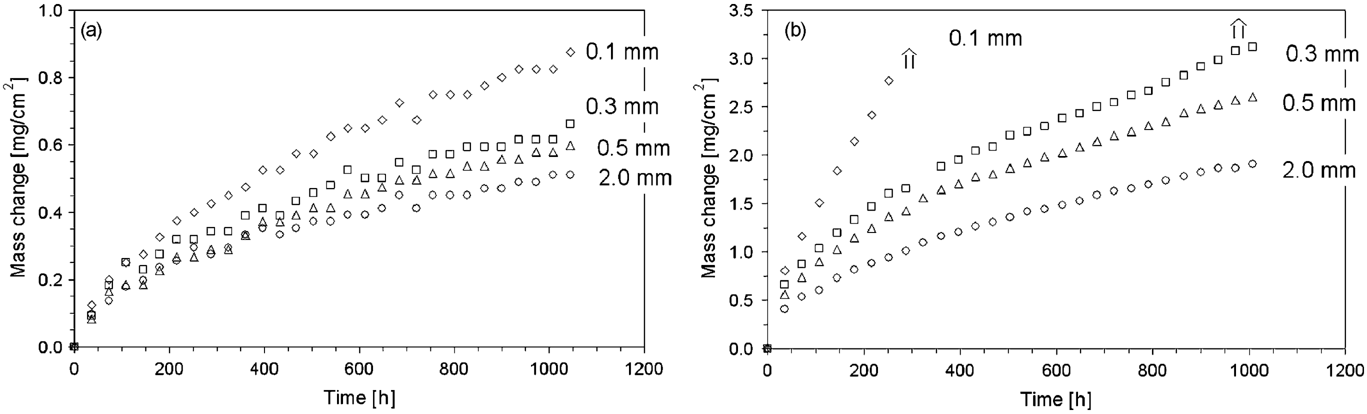

Fig. 1. Mass change during cyclic oxidation of high-Cr ferritic steel Crofer 22 APU in air for specimens of various thicknesses; (a) 800 °C and (b) 900 °C. Arrows indicate occurrence of breakaway oxidation [5].

model alloys was investigated at 1000 °C in synthetic and laboratory air and in Ar–H_2–H_2O gas mixtures.

2. Experimental

The studied materials were supplied by Thyssen Krupp VDM. The alloys were manufactured by vacuum melting 10 kg batches which were shaped into plates of 10 mm thickness by forging and hot rolling. The alloy compositions, analysed by inductively coupled plasma-optical emission spectroscopy (ICP-OES) and infrared (IR) analysis are listed in Table 1.

The alloy compositions were chosen in such a way, that in all studied cases real chromia-based surface scales are formed without substantial incorporation of transient, Ni-rich oxides. Mn was chosen as a ternary alloying element because most high temperature alloys contain Mn as a manufacturing related “impurity”, whereas the reactive element Y is frequently intentionally added to improve the alloy oxidation resistance.

For most of the oxidation experiments, samples of 20 mm × 10 mm × 2 mm were cut from the delivered plates and ground to a 1200 grit surface finish and ultrasonically cleaned in acetone immediately before use. In order to investigate the thickness dependence of the oxidation rate, specimens with a different initial thickness were used. For this purpose it was necessary to grind thick components to the required levels. For most of the “thickness dependence” experiments thick (~1.5 mm), medium (~0.5 mm) and thin (~0.2 mm) specimens were prepared.

Thermogravimetric measurements for up to 72 h exposure at 1000 °C were carried out in synthetic air using a Setaram Thermobalance (TG92). The total gas flow rates were 2 l/h, corresponding to a linear flow in the tubular reactor of 0.2 cm/s, at a total pressure of 1 bar. The individual samples were suspended on an alumina hook and gravimetric data were recorded continuously during each single experiment including the cooling of the specimen after the isothermal exposure. This procedure allowed not only measurement of the isothermal oxidation kinetics but also of any oxide scale spallation occurring during specimen cooling. The TG-results were corrected to account for buoyancy effects, using data measured for inert, alumina samples of the same geometry as the specimens used in the oxidation experiments.

The second group of experiments was carried out for up to 100 h exposure at 1000 °C in laboratory air and Ar–4%H_2–2%H_2O gas, in a horizontal furnace. Several specimens were placed in an alumina boat in a cold reactor tube. A preheated furnace was then moved over the specimens. The specimen temperature was measured by a thermocouple, which was located in the immediate vicinity of the specimen. In the case of Ar–4%H_2–2%H_2O, the furnace was equipped additionally with a glass tube. The samples were placed inside and the gas was generated by bubbling Ar–4%H_2 at atmospheric pressure through a saturator (humidifier) at room temperature. After flooding the furnace with the gas mixture, the hot furnace was moved over the samples. All specimens were weighed before and after oxidation exposure.

Table 1
Compositions of the investigated model alloys (mass%) determined by ICP-OES and IR spectroscopy

Alloy	Ni	Cr	Mn	Y	C	N	O	S
NiCr	Bal.	25	–	–	0.004	0.0023	0.017	0.001
NiCrY	Bal.	26.2	–	0.11	0.003	0.0021	0.0019	0.001
NiCrMn	Bal.	23.0	0.45	–	0.003	0.0017	0.018	0.001

The oxidized specimens were cross-sectioned and prepared for metallographic analysis using conventional techniques, i.e. grinding, polishing and fine polishing. Before mounting in an epoxy resin, the specimens were coated with a thin gold layer by sputtering, and subsequently by an electroplated Ni-layer. Analysis of oxide scale composition and morphologies was carried out using optical metallography, scanning electron microscopy (SEM) with energy dispersive X-ray analysis (EDX), wavelength dispersive X-ray analysis (WDX) and sputtered neutrals mass spectrometry (SNMS).

3. Results

Fig. 2 presents the results of TGA experiments on two alloys, NiCr and NiCrMn in synthetic air at 1000 °C. The mass gains for both alloys are observed to be progressively larger the thinner the specimen. These differences exist from the beginning of the exposures indicating that they are not associated with depletion of chromium or any other component from the alloys. Fig. 3 presents cross-sections of the scales on the thickest and thinnest of the NiCr TGA specimens. The scale on the 1.5-mm thick specimen is clearly much thinner than that on the 0.2-mm thick specimen, which is consistent with the mass change results in Fig. 2. Fig. 4 shows corresponding cross-section micrographs for the NiCrMn TGA specimens. Fig. 4 shows double-layered scales consisting mainly of an inner Cr_2O_3 layer and a thin layer of $MnCr_2O_4$ in the outer part of the scale. Also in this case the surface scale on the thin specimen is substantially larger than that on the thick specimen. The difference in scale thickness is mainly related to the difference in thickness of the inner chromia layer whereas the thickness of the outer spinel layer on the two specimens differs only marginally.

Fig. 5 presents Cr and Mn depletion profiles measured by WDX for specimens of NiCrMn alloy with different initial thickness after 72 h isothermal oxidation at 1000 °C in synthetic air. The data shows steep slopes of the depletion profile beneath the oxide scale. In spite of the scatter in data, the results indicate a